CIRSE

Fusion Guidance in Endovascular Peripheral Artery Interventions: A Feasibility Study

Anna M. Sailer · Michiel W. de Haan · Rick de Graaf ·
Willem H. van Zwam · Geert Willem H. Schurink ·
Patricia J. Nelemans · Joachim E. Wildberger · Marco Das

Abstract

Purpose   This study was designed to evaluate the feasibility of endovascular guidance by means of live fluoroscopy fusion with magnetic resonance angiography (MRA) and computed tomography angiography (CTA).

Methods   Fusion guidance was evaluated in 20 endovascular peripheral artery interventions in 17 patients. Fifteen patients had received preinterventional diagnostic MRA and two patients had undergone CTA. Time for fluoroscopy with MRA/CTA coregistration was recorded. Feasibility of fusion guidance was evaluated according to the following criteria: for every procedure the executing interventional radiologists recorded whether 3D road-mapping provided added value (yes vs. no) and whether PTA and/or stenting could be performed relying on the fusion road-map without need for diagnostic contrast-enhanced angiogram series (CEAS) (yes vs. no). Precision of the fusion road-map was evaluated by recording maximum differences between the position of the vasculature on the virtual CTA/MRA images and conventional angiography.

Results   Average time needed for image coregistration was 5 ± 2 min. Three-dimensional road-map added value was experienced in 15 procedures in 12 patients. In half of the patients (8/17), intervention was performed relying on the fusion road-map only, without diagnostic CEAS. In two patients, MRA roadmap showed a false-positive lesion. Excluding three patients with inordinate movements, mean difference in position of vasculature on angiography and MRA/CTA road-map was 1.86 ± 0.95 mm, implying that approximately 95 % of differences were between 0 and 3.72 mm (2 ± 1.96 standard deviation).

Conclusions   Fluoroscopy with MRA/CTA fusion guidance for peripheral artery interventions is feasible. By reducing the number of CEAS, this technology may contribute to enhance procedural safety.

A. M. Sailer (✉) · M. W. de Haan · R. de Graaf ·
W. H. van Zwam · J. E. Wildberger · M. Das
Department of Radiology, Maastricht University Medical
Center, Maastricht, The Netherlands
e-mail: anni.sailer@mumc.nl

M. W. de Haan
e-mail: m.de.haan@mumc.nl

R. de Graaf
e-mail: r.de.graaf@mumc.nl

W. H. van Zwam
e-mail: w.van.zwam@mumc.nl

J. E. Wildberger
e-mail: j.wildberger@mumc.nl

M. Das
e-mail: m.das@mumc.nl

G. W. H. Schurink
Department of Surgery, Maastricht University Medical Center,
Maastricht, The Netherlands
e-mail: gwh.schurink@mumc.nl

P. J. Nelemans
Department of Epidemiology, Maastricht University Medical
Centre, Maastricht, The Netherlands
e-mail: patty.nelemans@maastrichtuniversity.nl

M. Das
CARIM School for Cardiovascular Diseases, Maastricht
University Medical Center, Maastricht, The Netherlands

Introduction

Symptomatic peripheral artery disease (PAD) affects more than ten million people worldwide [1, 2]. Percutaneous transluminal angioplasty (PTA) with or without stent placement is a minimally invasive treatment option to restore arterial blood flow without need for open surgery. Contrast-enhanced magnetic resonance angiography (MRA) has gained broad acceptance in the preinterventional workup of patients and is performed routinely to diagnose PAD and to determine suitable treatment. If MRA is contraindicated or not available, contrast-enhanced computed tomography (CTA) is performed. During endovascular interventional procedures, diagnostic angiography with iodinated contrast medium (CM) is traditionally used to facilitate safe maneuvering of guidewires and catheters and to position angioplasty balloons and stents correctly. During the past decade, MR-guided interventions and coregistration of different imaging modalities have been promoted to facilitate multimodality fusion image road-mapping [3–7]. Recently, it has been shown that fusion image road-mapping can significantly reduce procedural CM volume in aneurysm repair and liver embolization [8–12]. To the best of our knowledge, fusion guidance in peripheral artery interventions has not been reported so far. This study was designed to evaluate the feasibility, precision, and added value of endovascular guidance by means of live fluoroscopy fusion with MRA and CTA.

Materials and Methods

The study was approved by the Institutional Ethical Committee. Written, informed consent was waived (METC 12-4-125). Fusion image road-mapping technology was evaluated in 20 endovascular peripheral artery interventions in 17 patients. Fifteen patients had undergone outpatient contrast-enhanced MRA of the iliac and lower leg arteries for diagnostic workup as published elsewhere [13] (Intera 1.5T, Philips Healthcare, Best, The Netherlands; 2D bolus tracking method, 15 ml Gadubotrol [Gadovist, Bayer Healthcare, Berlin, Germany; 7 ml Gd@1.2 ml/s—8.0 ml Gd@ 0.5 ml/s —followed by a saline chaser of 20 ml NaCl @ 0.5 ml/s]). In two patients with contraindications for MRA, contrast-enhanced CTA was performed (Somatom Definition, Siemens Healthcare, Forchheim, Germany; scan protocol: $2 \times 64 \times 0.6$-mm coll., pitch 0.9,

100/140 kV, quality ref. mAs 136/116 (+CareDose4D), rot. time 0.33 s, 1.0/0.8-mm slice reconstruction, soft tissue filter (D30f), 96 ml iopromide 300 [Ultravist, Bayer, Berlin, Germany; (flow rate 4.8 ml, IDR = 1.44 gI/s)]. Timing interval between the MRA/CTA acquisition and endovascular procedure was up to 8 weeks.

Volumetric datasets of the pre-procedurally acquired MRA and CTA images were loaded to a commercially available 3D image fusion workstation (Allura XtraVision 8.3, Philips). Patients were placed in a supine position on the angiography unit's table comparable to the position during MRA and CTA acquisition. Flat panel detector C-arm cone-beam CT (CBCT) (Allura Xper FD20, Philips) of the pelvic or upper leg region was acquired right before draping the patient. Volumetric CBCT datasets were automatically transferred to the 3D workstation. Coregistration of the preacquired MRA/ CTA datasets to the CBCT datasets was performed manually by the interventional radiologists. Figure 1 shows the procedure of dataset coregistration. Vessels, corresponding vessel wall calcifications, bones, and organ borders visible on both datasets were used as landmarks for registration and were verified in three dimensions. By these means, the MRA/CTA datasets were linked to the 3D coordinate space of the C-arm and the corresponding live fluoroscopy image. Dataset coregistration persisted during the entire procedure; the MRA/CTA volume thereby followed any rotation of the C-arm as well as table movements and is adapted to magnification. Guidewires, catheters, PTA balloons, and stents were overlaid to the MRA/CTA vessel tree background allowing noncontrast enhanced endovascular road-mapping. By means of manually window leveling, the vasculature of the MRA dataset could be made clearly visible with reduced artifacts from bone and soft tissue structures. Bone removal enhanced the vessel tree on the CTA dataset.

Patients and Procedures

Fluoroscopy with MRA/CTA fusion road-map technology was evaluated in 14 common and/or external iliac artery interventions and six superficial femoral artery and/or popliteal artery interventions in 17 patients. Patients with below-the-knee lesions and patients who had undergone diagnostic imaging longer than 8 weeks ago were not included. Interventions were performed under local anesthesia. A detailed description of the included patients, clinical presentations, and vascular pathology on imaging is given in Table 1. Figures 2, 3 and 4 show application of fusion road-mapping in various procedures.

Fusion Road-Map Evaluation

Time for C-arm CBCT with MRA/CTA dataset coregistration (in minutes) was monitored. Feasibility of fusion

Fig. 1 Manually performed rigid coregistration of the volumetric contrast-enhanced MRA dataset (*left*) and CBCT dataset (*right*) by bringing aortic bifurcation and corresponding vessel wall calcifications into the crosshair. MRA and CBCT image coregistration is further adjusted in axial and sagittal planes (not shown) using vessel borders, bone structures, and muscles as landmarks
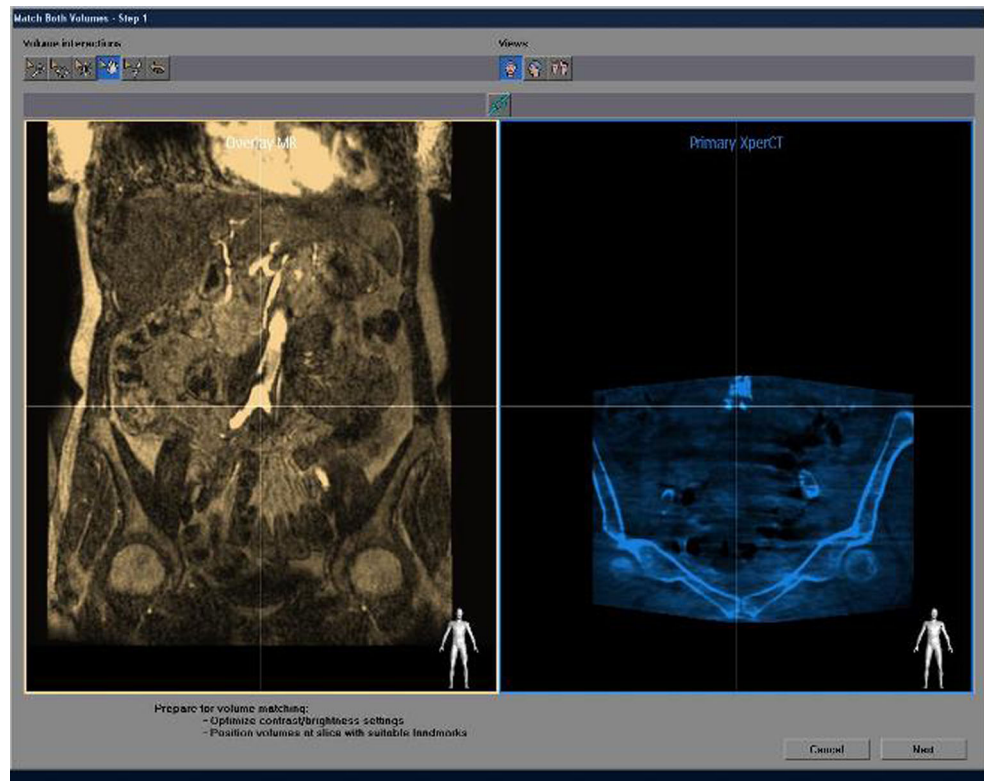
Table 1 Overview of included patients and their clinical presentation and corresponding contrast-enhanced MRA and CTA findings

Patient ID	Sex	Age	Clinical presentation	MRA/CTA diagnosis
1	Male	86	Fontaine 2B claudication left leg	MRA: Severe stenosis left AIC and AIE over five cm length
				MRA: Severe aortic bifurcation stenosis with occlusion right
2	Female	77	Fontaine 3 bilateral buttock claudication	AIC > 2 cm length (1) and severe stenosis left AIC > 5 cm length (2)
3	Female	59	Fontaine 2B claudication left leg	MRA: Occlusion left AIE of 1 cm length
4	Male	67	Fontaine 2B both legs	MRA: Severe stenosis right proximal AIC
5	Male	68	Fontaine 3 claudication both legs	MRA: Occlusion left SFA of 22 cm length
6	Male	72	Fontaine 3 claudication right leg	MRA: Severe stenosis right popliteal artery of 3 cm length
7	Female	68	Fontaine 2B claudication right buttock	CTA: Occlusion right AIE of 4 cm length and severe in-stent stenosis right AIC
8	Female	45	Fontaine 2B claudication bilateral buttock	MRA: Severe stenosis left AIC (1) of 5 cm length and right AIC (2) of 3 cm length
9	Female	60	Fontaine 2B claudication left leg	MRA: Severe stenosis left AIC of 2 cm length
10	Male	68	Fontaine 2B claudication right leg	CTA: Occlusion and dissection left AIE of 5 cm length
11	Male	54	Fontaine 2B claudication left leg more than right leg	MRA: Severe stenosis left AIE of 3 cm length (1) and severe stenosis right distal SFA of 4 cm length (2)
12	Female	59	Fontaine 2B claudication left leg	MRA: Occlusion left SFA of 14 cm length
13	Male	67	Fontaine 3 claudication left leg	MRA: Occlusion left SFA of 2 cm length, severe stenosis whole popliteal artery and tibiofibular trunk origin
14	Male	75	Fontaine 3 claudication left leg	MRA: Occlusion and severe stenosis left AIE and AIC of 9 cm length
15	Male	69	Fontaine 3 claudication left leg	MRA: Multiple severe stenoses and occlusions whole left SFA
16	Female	62	Fontaine 3 claudication left leg	MRA: Occlusion whole left AIE and stenosis left AIC of 4 cm length
17	Female	88	Fontaine 2B claudication left leg	MRA: Severe stenosis left AIE of 2 cm length

AIC common iliac artery, *AIE* external iliac artery, *SFA* superficial femoral artery
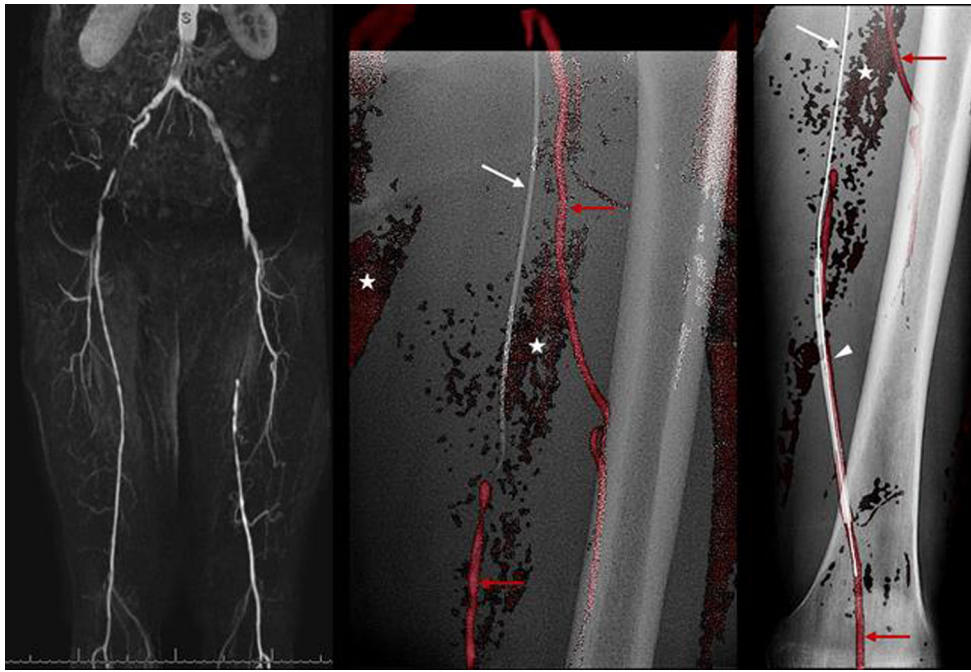
Fig. 2 Contrast-enhanced MRA image (*left*) in patient 12 shows long distance occlusion of the *left* proximal superficial femoral artery (SFA). Artifacts from previously placed stent in the distal aorta and occlusion of the *right* external iliac artery are visible. Live fluoroscopy overlay (*grey*) to the MRA dataset (background) allows noncontrast usage 3D road mapping during SFA recanalization (*middle*) and balloon angioplasty (*right*). Guidewire (*white arrows*) and PTA balloon (*white arrow head*) superimposed on the MRA vessel tree (*red arrows*). Artifacts from upper leg muscles (*stars*), partly removed from the MRA dataset by window-leveling
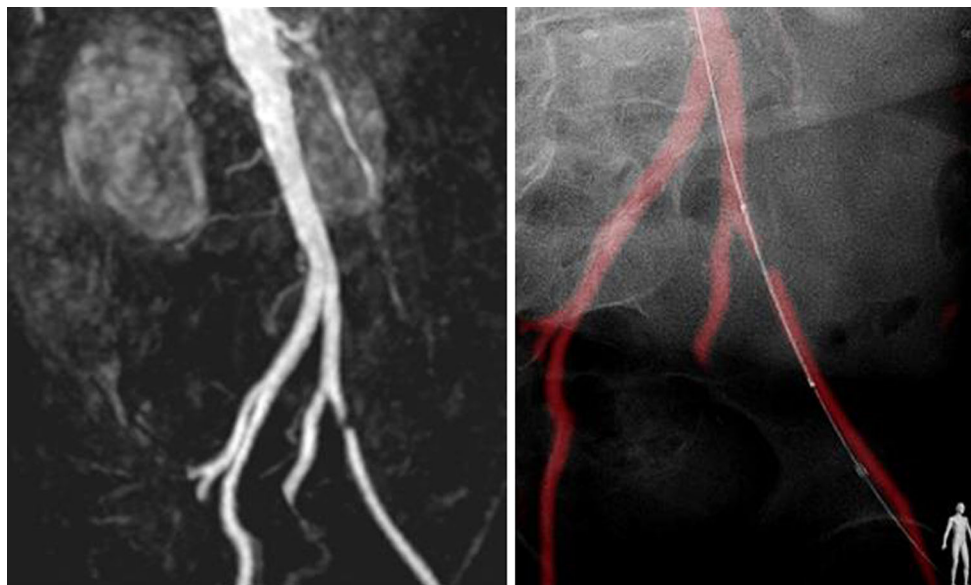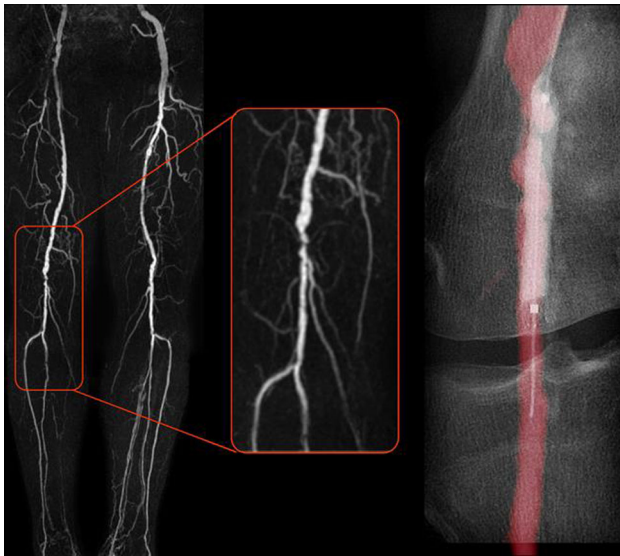

Fig. 3 Contrast-enhanced MRA image (*left*) in patient 3 shows a short occlusion of the *left* AIE. Direct retrograde access for *left* external iliac artery recanalization and balloon angioplasty based on fusion road-mapping without further need of CM. C-arm in 40 degrees right lateral position and fusion road-map following the 3D projection of live fluoroscopy. Conventional post-PTA control angiography was performed and indicated need for additional stent placement

guidance was evaluated according to the following criteria: (1) For every procedure the executing interventional radiologists recorded whether 3D road-mapping provided added value in terms of defining the best C-arm projection angle for the particular intervention (yes vs. no) and whether PTA and/or stenting could be performed relying

Fig. 4 Contrast-enhanced MRA image (*left*) in patient 6 shows a stenosis of the right popliteal artery. PTA balloon positioning and deployment based on the fusion road-map (*right*) without need for additional diagnostic CM-enhanced angiogram

on the fusion road-map without the need for a diagnostic contrast enhanced angiogram series (CEAS) (yes vs. no). Subjective scores were documented by the interventional radiologists using a standardized online data registration form right after the procedure. (2) Precision of the MRA/CTA with fluoroscopy fusion road-map was evaluated by recording differences between the position of the vasculature on the virtual MRA/CTA images and conventional angiography. Displacement of the fusion road map was measured as the maximum mismatch in the region of interest (ROI) in millimetres using the measurement tool of the 3D workstation subsequently to each procedure. In patients in whom there was no need to perform a diagnostic angiogram before treatment, the fusion roadmap was compared with the control angiogram that was made after treatment.

Results

Average time needed for dataset coregistration was 5 ± 2 min (mean $\pm$ standard deviation). Fusion road-map added value was experienced in 15 procedures (75 %) in 12 patients. In three procedures, inordinate patient movement after CBCT acquisition hindered the use of the fusion road-map. In the procedures of patients 4 and 17, the diagnostic MRA and corresponding fusion road-map indicated a severe stenosis of the right common iliac artery (AIC) and left external iliac artery (AIE), respectively. The vessel section could be easily passed with the guidewire and conventional angiography was performed to visualize the

extent of the stenosis. In both patients, on two directional conventional angiography series, no stenosis was visible and no intervention was performed. In 47 % of the patients (8/17) PTA and/or stenting could be performed relying on the fusion road-map and a diagnostic CEAS was not required. Average maximum difference in position of vasculature on angiography and MRA/CTA fusion road-map was 6.41 mm with a standard deviation of 11.12 mm. Excluding the three patients with major leg and pelvis movement during the procedure, average maximum difference was 1.86 ± 0.95 mm, which implies that approximately 95 % of differences were between 0 and 3.72 mm (2 ± 1.96 standard deviation). Distribution of 3D road-map added value and precision per patient is shown in Table 2.

Discussion

Fusion guidance is a new technology for endovascular road-mapping. Flat panel detectors that can acquire rotational volumetric datasets for image coregistration are increasingly replacing conventional fluoroscopy units and coregistration software is commercially available from different vendors. To our knowledge, we are the first to report fluoroscopy coregistration with MRA/CTA for the application of peripheral artery interventions. In our series, dataset coregistration with MRA or CTA was feasible in all procedures. Coregistration was performed by the interventional radiologist on the 3D workstation while further preparations inside the angiography suite (draping the patient, preparing the table) were performed by the nurses. Actual time loss for fusion road-mapping therefore was negligible.

Conventional catheter road-mapping with iodinated CM has potential nephrotoxic side-effects, which are correlated with the amount of CM and therefore should be regarded as relevant in patients with renal impairment and diabetes, both associated with PAD [1, 14, 15]. Furthermore, endovascular interventions with angiography are contraindicated in patients with serious allergy to CM. Any technology to reduce procedural CM is therefore of high importance [16].

Previously, Manke et al. [17] outlined the feasibility of MR guided iliac artery stenting in 13 patients. Real-time monitoring by live fluoroscopy was lacking, which resulted in long procedure time. Metal artifacts on MR further restricted applicability for routine clinical practice. These limitations are addressed by fusion technology, which links the preinterventional MRA/CTA information to dynamic fluoroscopy. As volumetric MRA or CTA datasets are registered, the vessel tree follows any three-dimensional

Table 2 Overview of characteristics of endovascular procedures

Patient ID	Intervention	Fusion road-map precision (mm)	Added value by 3D road-map	Added value by diagnostic CEAS reduction	Amount of iodinated contrast reduction (CEAS series) (cc)	Total procedural iodinated contrast material (cc)	Total procedure time (min)
1	Retrograde PTA and stenting left AIC and AIE	2	Yes	Yes	15	30	45
2	Bilateral retrograde stenting distal aorta and left and right AIC	2	Yes	Yes	15	60	100
3	Retrograde recanalization and stenting left AIE	1	Yes	Yes	15	40	100
4	Retrograde access right AFC. Angiography shows no stenosis. No intervention performed. Diagnostic angiography of the whole right leg performed	1	No	No		90	65
5	Trial for antegrade recanalization SFA, not successful	Patient movement, 42	No	No		45	105
6	Antegrade PTA and stenting right popliteal artery	1	Yes	Yes	6	55	55
7	Retrograde recanalization and stenting right AIE and PTA right AIE	Patient movement, 18	No	No		70	60
8	Bilateral retrograde PTA left and right AIC	3	Yes	No		50	60
9	Retrograde stenting left AIC	1	Yes	No		50	50
10	Retrograde recanalization and stenting right AIE	2	Yes	No		40	90
11	Retrograde PTA left AIE and over the bifurcation PTA right SFA	1	Yes	Yes	15	65	100
12	Antegrade recanalization and stenting left SFA	1	Yes	Yes	6	50	100
13	Antegrade recanalization and stenting left SFA, PTA popliteal artery and tibiofibular trunk	2	Yes	Yes	12	125	260
14	Retrograde recanalization, PTA and stenting left AIC and AIE	Patient movement, 23	No	No		70	155
15	Trial for antegrade recanalization SFA, not successful	3	Yes	No		40	165
16	Retrograde recanalization and stenting left AIE and PTA left AIC	2	Yes	Yes	15	70	155
17	Retrograde access left AFC. Conventional angiogram shows patent left iliac arteries. No intervention performed	4	No	No		40	70

PTA percutaneous transluminal angioplasty, *AIC* common iliac artery, *AIE* external iliac artery, *SFA* superficial femoral artery

C-arm rotation. Optimal projection angles can be chosen while rotating the C-arm under fluoroscopy.

In a previously reported case, thoracic aortic repair without CM administration has been performed [8]. In our study, PTA and/or stenting without a pretreatment CEAS, so fully relying on the fusion road-map, was performed in half of the patients; in the other half, however, we still needed support from an angiogram. Posttreatment control angiograms were further performed in all patients to analyze success of the intervention and to detect possible complications; we therefore did not perform procedures without CM administration. Still the reduction of preinterventional angiograms in eight patients shows that fusion guidance technology holds the potential for CM reduction in future procedures, which could be especially relevant for patients with renal impairment. In patients with severe allergy to iodinated contrast material, zero-iodinated-contrast interventions might be possible in combination with ultrasound control or low volume of gadolinium or carbon dioxide. Further trials—ideally prospective, randomized trials—are necessary to prove the concept of contrast saving by image fusion and to determine effects quantitatively on procedural contrast usage in a broad patient population.

Dataset coregistration requires acquisition of a CBCT. The staff is usually outside the angiosuite during acquisition, but extra radiation dose for the patient has to be considered. Mean patients' radiation dose in terms of dose are product (DAP) from CBCT in the pelvic region was 14.5 $Gycm^2$ [95 % confidence interval (CI) 11.6–17.4 $Gycm^2$], which accounted on average for 21.4 % (95 % CI 16.4–26.2 %) of the total procedural DAP. Calculated maximum risk for lifetime exposure induced cancer death is less than 0.03 % in pelvic CBCT [18]. For the PAD patient population, potential benefit from contrast savings by use of fusion road-mapping might overweight the negative impact of the extra radiation dose. However, this has to be judged by the interventional radiologist individually for each case under consideration of patient's renal function and age.

Main limitations of fusion road-mapping are patient movement and MRA artifacts. Similar to conventional road mapping, any patient movement after CBCT acquisition results in mismatch of the fusion road-map. In 18 % of the patients (3/17), inordinate (rotational) movements inhibited the use of the fusion road-map—a limitation that needs to be addressed for further application, e.g., by immobilization pelvis and legs casts. Furthermore, different patient positioning in preinterventional imaging and interventional procedure should be considered as this might have affected fusion road-map precision. The results of this study indicate that—except for the patients with major movement during the procedure—differences between position of vasculature on angiography and MRA/CTA fusion road-map did not exceed four millimeters. Most of the procedures were iliac interventions. Displacements of such magnitude might be considered acceptable for adequate balloon and stent positioning in most peripheral artery applications, especially in those with larger vessel regions. As was shown in our study, no complications were detected even in those interventions ($n = 8$), which were performed solely relying on fusion road-mapping. Furthermore, minor displacement of the fusion road-map can be corrected manually during the procedure by readjusting the MRA/CTA dataset on fluoroscopy landmarks, e.g., a catheter placed over the aortic bifurcation and other landmarks visible under fluoroscopy. However, for anatomic regions with smaller vessel diameters, recanalization procedures, and stenting nearby side branches, potential risk of device misplacement has to be taken serious and might inhibit application of this technology as long as precision is not further improved. In terms of diagnostic accuracy, one must realize that the fusion image road-map is only as accurate as the underlying MRA or CTA quality as artifacts hamper the usability of the fusion road-map. Also timing intervals between MRA acquisition and PTA/stenting procedure might cause inaccuracies. In two of the studied patients, the diagnostic MRA indicated a false-positive (severe) stenosis of the left iliac artery. This error was detected on an additional conventional angiogram and might have resulted in unnecessary PTA if evaluation with conventional angiogram would not have been performed. However, imaging techniques such as CTA and MRA are constantly improving and the number of pseudo lesions decreases. In a recent meta-analysis by Jens et al. [19] it was shown that both CTA and MRA are highly accurate with sensitivity of 96 and 93 % and specificity of 95 and 94 % respectively; still, potential risk of pseudo lesions always needs to be considered when using fusion road-mapping.

In conclusion, fusion of preinterventional MRA and CTA datasets with live fluoroscopy for real-time 3D road-mapping in endovascular peripheral artery interventions is feasible. The technology holds potential to reduce contrast dosage and may contribute to enhance renal safety.

References

1. Selvin E, Erlinger TP (2004) Prevalence of and risk factors for peripheral arterial disease in the United States: results from the national health and nutrition examination survey, 1999–2000. Circulation 110(6):738–743

2. Harris K (2008) The worldwide burden of peripheral artery disease. Inter-society consensus for the management of peripheral artery disease (TASC II). Available at: http://www.radiolodzy-interwencyjni.pl/forms/961.pdf. Accessed 24 Nov 2013

3. Raval AN, Karmarkar PV, Guttman MA, Ozturk C, Sampath S, DeSilva R, Aviles RJ, Xu M, Wright VJ, Schenke WH, Kocaturk O, Dick AJ, Raman VK, Atalar E, McVeigh ER, Lederman RJ (2006) Real-time magnetic resonance imaging-guided endovascular recanalization of chronic total arterial occlusion in a swine model. Circulation 113(8):1101–1107

4. Buecker A, Adam GB, Neuerburg JM, Kinzel S, Glowinski A, Schaeffter T, Rasche V, van Vaals JJ, Guenther RW (2002) Simultaneous real-time visualization of the catheter tip and vascular anatomy for MR-guided PTA of iliac arteries in an animal model. J Magn Reson Imaging 16(2):201–208

5. Fink C, Bock M, Umathum R, Volz S, Zuehlsdorff S, Grobholz R, Kauczor HU, Hallscheidt P (2004) Renal embolization: feasibility of magnetic resonance-guidance using active catheter tracking and intraarterial magnetic resonance angiography. Invest Radiol 39(2):111–119

6. Klein AJ, Tomkowiak MT, Vigen KK, Hacker TA, Speidel MA, Vanlysel MS, Shah N, Raval AN (2012) Multimodality image fusion to guide peripheral artery chronic total arterial occlusion recanalization in a swine carotid artery occlusion model: unblinding the interventionalist. Catheter Cardiovasc Interv 80(7):1090–1098

7. van der Hoeven BL, Schalij MJ, Delgado V (2012) Multimodality imaging in interventional cardiology. Nat Rev Cardiol 9(6):333–346

8. Kobeiter H, Nahum J, Becquemin JP (2011) Zero-contrast thoracic endovascular aortic repair using image fusion. Circulation 124(11):e280–e282

9. Dijkstra ML, Eagleton MJ, Greenberg RK, Mastracci T, Hernandez A (2011) Intraoperative C-arm cone-beam computed tomography in fenestrated/branched aortic endografting. J Vasc Surg 53(3):583–590

10. Sailer AM, de Haan MW, Peppelenbosch AG, Jacobs MJ, Wildberger JE, Schurink GW (2014) CTA with fluoroscopy image fusion guidance in endovascular complex aortic aneurysm repair. Eur J Vasc Endovasc Surg 47(4):349–356

11. Sadek M, Berland TL, Maldonado TS, Rockman CB, Mussa FF, Adelman MA, Veith FJ, Cayne NS (2014) Use of preoperative magnetic resonance angiography and the Artis zeego fusion program to minimize contrast during endovascular repair of an iliac artery aneurysm. Ann Vasc Surg 28(1):261.e1–5

12. Bargellini I, Turini F, Bozzi E, Lauretti D, Cicorelli A, Lunardi A, Cioni R, Bartolozzi C (2013) Image fusion of preprocedural CTA with real-time fluoroscopy to guide proper hepatic artery catheterization during transarterial chemoembolization of hepatocellular carcinoma: a feasibility study. Cardiovasc Intervent Radiol 36(2):526–530

13. Versluis B, Backes WH, van Eupen MG, Jaspers K, Nelemans PJ, Rouwet EV, Teijink JA, Mali WP, Schurink GW, Wildberger JE, Leiner T (2011) Magnetic resonance imaging in peripheral arterial disease: reproducibility of the assessment of morphological and functional vascular status. Invest Radiol 46(1):11–24

14. Romero JM, Bover J, Fite J, Bellmunt S, Dilmé JF, Camacho M, Vila L, Escudero JR (2012) The modification of diet in renal disease 4-calculated glomerular filtration rate is a better prognostic factor of cardiovascular events than classical cardiovascular risk factors in patients with peripheral arterial disease. J Vasc Surg 56(5):1324–1330

15. Hölscher B, Heitmeyer C, Fobker M, Breithardt G, Schaefer RM, Reinecke H (2008) Predictors for contrast media-induced nephropathy and long-term survival: prospectively assessed data from the randomized controlled Dialysis-Versus-Diuresis (DVD) trial. Can J Cardiol 24(11):845–850

16. Laskey WK, Jenkins C, Selzer F, Marroquin OC, Wilensky RL, Glaser R, Cohen HA, Holmes DR Jr (2007) NHLBI Dynamic Registry Investigators. Volume-to-creatinine clearance ratio: a pharmacokinetically based risk factor for prediction of early creatinine increase after percutaneous coronary intervention. J Am Coll Cardiol 50(7):584–590

17. Manke C, Nitz WR, Djavidani B, Strotzer M, Lenhart M, Völk M, Feuerbach S, Link J (2001) MR imaging-guided stent placement in iliac arterial stenoses: a feasibility study. Radiology 219(2):527–534

18. Sailer AM, Schurink GWH, Wildberger JE, de Graaf R, van Zwam WH, de Haan MW, Kemerink GJ, Jeukens CRLPN (2014) Radiation exposure of abdominal cone beam computed tomography. Cardiovasc Interv Radiol. doi:10.1007/s00270-014-0900-7

19. Jens S, Koelemay MJ, Reekers JA, Bipat S (2013) Diagnostic performance of computed tomography angiography and contrast-enhanced magnetic resonance angiography in patients with critical limb ischaemia and intermittent claudication: systematic review and meta-analysis. Eur Radiol 23(11):3104–3114